

## Large Glass-forming Ability and Magnetocaloric Effect in $Gd_{55}Co_{20}Al_{23}Si_2$ Bulk Metallic Glass

Li Qian<sup>1</sup>, Cai Pingping<sup>1</sup>, Shen Baolong<sup>1\*</sup>, Makino Akihiro<sup>2</sup>, and Inoue Akihisa<sup>2</sup>

<sup>1</sup>Ningbo Institute of Materials Technology & Engineering, Chinese Academy of Sciences, Ningbo 315201, China

<sup>2</sup>Institute for Materials Research, Tohoku University, Sendai, Japan

(Received 21 August 2011, Received in final form 13 October 2011, Accepted 14 October 2011)

**In this study, we investigated the glass-forming ability (GFA) and magnetocaloric effect (MCE) of  $Gd_{55}Co_{20}Al_{23}Si_2$  bulk glassy alloy. It is found that the addition of 2 at% Si is effective for extension of the supercooled liquid region ( $\Delta T_x$ ), the  $\Delta T_x$  is 55 K for the  $Gd_{55}Co_{20}Al_{25}$  glassy alloy, and increases to 79 K for the  $Gd_{55}Co_{20}Al_{23}Si_2$  alloy. As a result,  $Gd_{55}Co_{20}Al_{23}Si_2$  glassy alloys with diameters up to 5 mm were successfully synthesized. The alloys also exhibit large MCE, i.e., the magnetic entropy change ( $\Delta S_m$ ) of  $8.9 \text{ J kg}^{-1} \text{ K}^{-1}$ , the full width at half maximum of the  $\Delta S_m$  ( $\delta T_{FWHM}$ ) of 87 K, and the refrigerant capacity (RC) of  $774 \text{ J kg}^{-1}$ .**

**Keywords :** Gd-based bulk glassy alloys, glass-forming ability, magnetocaloric effect, magnetic entropy change

### 1. Introduction

Magnetic materials exhibiting large magnetocaloric effect (MCE) have been drawing increasing attention due to their potential application as magnetic refrigerants [1, 2]. Compared with traditional vapor-compression refrigeration, the magnetic refrigerants exhibit advantages both of environmental friendliness and relatively high efficiency [3]. Magnetic refrigeration is a cooling technology based on the magnetocaloric effect. For a magnetic material exhibiting MCE, the alignment of randomly oriented magnetic moments by an external magnetic field results in the reduction of the magnetic entropy of the material. When the magnetic field is subsequently turned off, the magnetic moments randomize again, which conversely leads to cooling effect [4]. Usually, the magnetic materials have large enough spontaneous magnetization and a strong temperature dependence of magnetization around its phase transition temperature to obtain large MCE [5]. Currently, a series of materials with large isothermal magnetic entropy change ( $\Delta S_M$ ) have been found, such as  $Gd_5(Si,Ge)_4$  [1],  $Ni_2MnGa$  [6],  $La(Fe,Si)_{13}$  [7],  $MnAs$  [8],  $MnFe(P,As)$  [2], etc.

In recent years, the study of magnetic refrigeration has been increasing focused on amorphous magnetic materials

with a second-order phase transition due to their intrinsic nature, such as the tailorable nature of the ordering temperature, high electrical resistivity, low hysteresis loss, and high corrosion resistance. Previous work revealed that amorphous magnetic materials exhibit large magnetic entropy changes comparable to that of some known crystalline magnetic refrigerants. Further more, the amorphous materials have a larger temperature range of the half maximum peak of  $\Delta S_M$  and that lead to a much higher refrigerant capacity (RC), which is another important parameter to evaluate the technological interest in a refrigerant material [9]. Very recently, a series of Gd-based bulk glassy alloys (BGAs) with large MCE have been developed, such as  $Gd_{60}Co_{26}Al_{14}$  [10],  $Gd_{55}Co_{20}Al_{25}$  [11],  $Gd_{36}Y_{20}Al_{24}Co_{20}$  [12]  $Gd_{53}Al_{24}Co_{20}Zr_3$  [4], etc. However, a major challenge for these BGAs is their limited glass-forming ability (GFA). Large GFA often combine with high thermal stability and high crystallization resistance. This makes glassy alloys easy to scale product and to maintain good properties for a long time. In this work, based on above considerations, new composition of bulk glassy alloy  $Gd_{55}Co_{20}Al_{24}Si_2$  with good GFA and MCE has been synthesized. It is found that the addition of only 2 at.% Si is efficiently for extension the GFA of  $Gd_{55}Co_{20}Al_{25}$ , and the MCE is also slightly improved.

\*Corresponding author: Tel: (+86)574-87911392  
e-mail: blshen@nimte.ac.cn

## 2. Experiments

The Gd-based BGAs with a nominal composition of  $\text{Gd}_{55}\text{Co}_{20}\text{Al}_{23}\text{Si}_2$  was prepared by arc-melting Gd (99.9%), Co (99.99%), Al (99.99%), Si (99.99%) in Ti-gettered argon atmosphere. The ingot was remelted 5 times and suck cast into a Cu mold to get a cylindrical rod of 5 mm in diameter. Their structure were ascertained by powder X-ray diffraction (XRD) with Cu  $K\alpha$  radiation at 40 kV. Thermal analysis was carried out by differential scanning calorimetry (DSC) at a heating rate of 40 K  $\text{min}^{-1}$  and a cooling rate of 4 K  $\text{min}^{-1}$ . The temperature and field dependences of magnetization were measured by physical properties measurement system (ppms).

## 3. Results and Discussion

Fig. 1 shows the XRD pattern of the as-cast  $\text{Gd}_{55}\text{Co}_{20}\text{Al}_{23}\text{Si}_2$  rod. Only broad peaks without crystalline peak can be seen for the bulk sample, which indicate the formation of a glassy phase in the diameter of 5 mm.

The glass nature of  $\text{Gd}_{55}\text{Co}_{20}\text{Al}_{23}\text{Si}_2$  was also confirmed by the DSC measurement at a heating rate of 40 K  $\text{min}^{-1}$  as shown in Fig. 2. The distinct glass transition and sharp crystallization verify the glassy structure of the alloy. The values of glass transition temperature ( $T_g$ ) and the onset crystallization temperature ( $T_x$ ) are 600 K and 679 K, respectively. The DSC curve with a cooling rate of 4 K  $\text{min}^{-1}$  of the alloy is shown in the inset of Fig. 2. The liquidus temperature  $T_l$  is determined to be 957 K. The supercooled liquid region ( $\Delta T_x = T_x - T_g$ ) and reduced glass transition temperature  $T_{rg}$  ( $T_{rg} = T_g/T_l$ ), which are two important parameters in determining the GFA of an

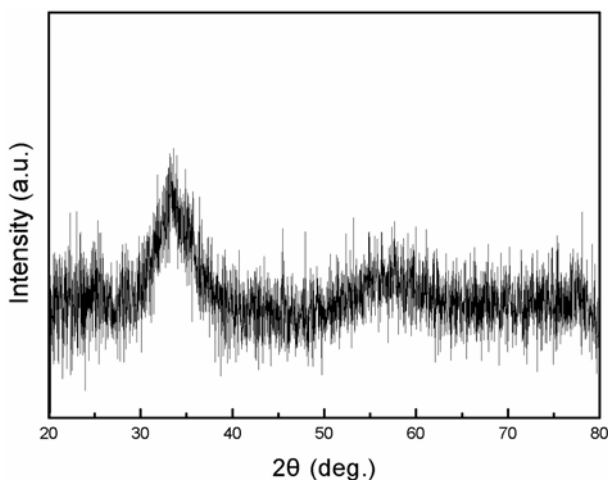


Fig. 1. The powder XRD pattern of the cast  $\text{Gd}_{55}\text{Co}_{20}\text{Al}_{23}\text{Si}_2$  alloy rod with critical diameter of 5 mm.

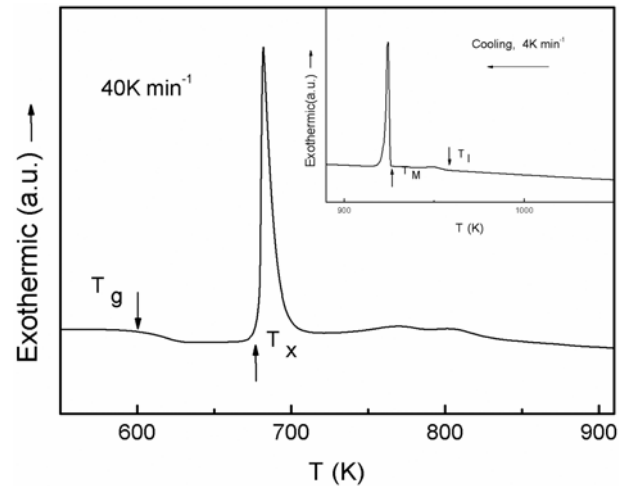
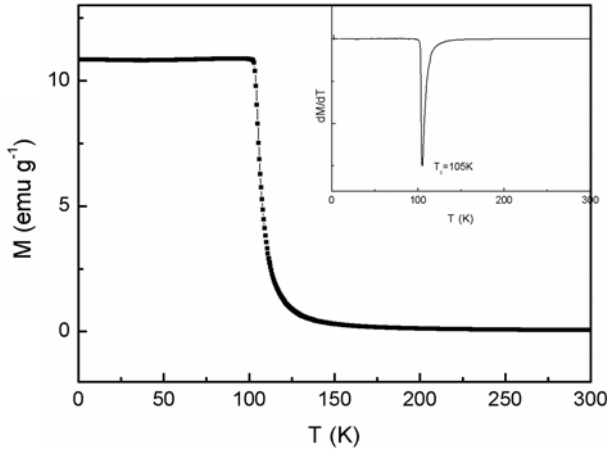


Fig. 2. The DSC curve of the cast  $\text{Gd}_{55}\text{Co}_{20}\text{Al}_{23}\text{Si}_2$  alloy rod (the heating rate is 40 K  $\text{min}^{-1}$ ). The inset shows the DSC curve with a cooling rate of 4 K  $\text{min}^{-1}$ .

alloy, are 79 K and 0.63, respectively. Compared with  $\text{Gd}_{55}\text{Co}_{20}\text{Al}_{25}$  alloy ( $\Delta T_x = 55$  K<sup>11</sup> and  $T_{rg} = 0.61$  [13]), the  $\Delta T_x$  and  $T_{rg}$  of  $\text{Gd}_{55}\text{Co}_{20}\text{Al}_{23}\text{Si}_2$  alloy have increased 13 K and 0.02, which indicate the enhancement of the stability of the undercooled melt, and lead to a better GFA.

Here we discuss the reason why the GFA of Gd-based glassy alloy is enhanced by Si addition. The atomic radii of Gd, Co, Al and Si are 0.178, 0.125, 0.143 and 0.117 nm, respectively [14]. Only Si atom holds the smallest atomic radius, which is 0.117 nm. Poon have pointed out that the large (L) and small (S) atoms may form a strong L-S percolating network or reinforce “backbone” in the amorphous structure, and presumably, the backbone structure can enhance the stability of the undercooled melt which suppresses crystallization [15]. The enthalpy of mixing is  $-56$  kJ  $\text{mol}^{-1}$  for the Gd-Si pair,  $-21$  kJ  $\text{mol}^{-1}$  for the Co-Si pair,  $-38$  kJ  $\text{mol}^{-1}$  for the Gd-Al pair,  $-19$  kJ  $\text{mol}^{-1}$  for the Co-Al pair and  $-2$  kJ  $\text{mol}^{-1}$  for the Al-Si pair [16]. It can be seen that the mixing enthalpies with negative values of the atomic pairs between Si and Gd or Co are larger than those of the atomic pairs between Al and Gd or Co, respectively. It has been reported for the bulk glassy alloys that the satisfaction of the three component rules, i.e., (1) multicomponent, (2) significant atomic size mismatches, and (3) negative heats of mixing, therefore the Si addition can lead to a better GFA.

Fig. 3 shows the temperature dependence of the magnetization  $M(T)$  for  $\text{Gd}_{55}\text{Co}_{20}\text{Al}_{23}\text{Si}_2$  alloy measured in an applied field of 200 Oe. The inset in Fig. 3 exhibits the  $dM/dT$  versus temperature curve. The value of Curie temperature ( $T_c$ ), determined as the temperature corresponding to the minimum in  $dM/dT$ , is 105 K. As it is



**Fig. 3.** Temperature dependence of the magnetization in a magnetic field of 200 Oe for the Gd<sub>55</sub>Co<sub>20</sub>Al<sub>23</sub>Si<sub>2</sub> BGA.

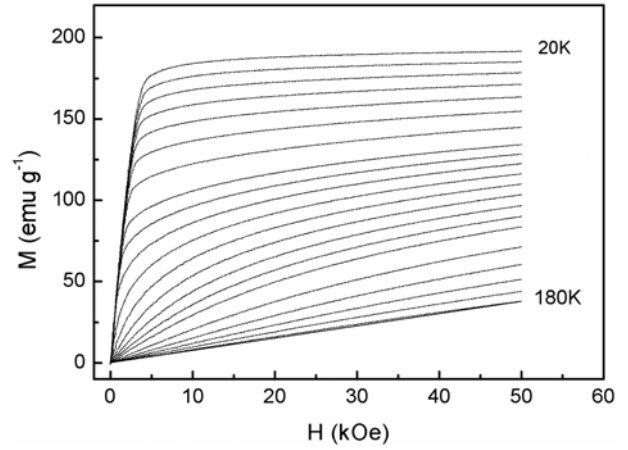


**Fig. 4.** Isothermal magnetization as a function of magnetic field at various temperatures.

noted from Fig. 3, the magnetization varies rapidly around the magnetic-ordering temperature. According to the Maxwell relation, a large magnetic entropy may be expected.

Isothermal magnetization curves of  $M-H$  with an increasing field at different temperatures are displaced in Fig. 4. A temperature interval of 5 K and 10 K was chosen for the regions near  $T_c$  and far away from  $T_c$  respectively. The sweeping rate of the field was slow enough to ensure that the data were recorded in an isothermal process. The magnetic entropy ( $\Delta S_m$ ) of Gd<sub>55</sub>Co<sub>20</sub>Al<sub>23</sub>Si<sub>2</sub> alloy is calculated by Maxwell relation,

$$\Delta S_m = \int_{H_{\min}}^{H_{\max}} \left( \frac{\partial M}{\partial T} \right) dH \quad (1)$$

where  $H_{\min}$  ( $H_{\min}$  is usually fixed to zero) and  $H_{\max}$  are the initial and final values of magnetic field respectively, and maximal value is 50 kOe in our experiments. By Eq. (1), the temperature dependence of  $\Delta S_m$  for Gd<sub>55</sub>Co<sub>20</sub>Al<sub>23</sub>Si<sub>2</sub> alloy in the applied field of 50 kOe are obtained (shown in Fig. 5). The peak values of  $-\Delta S_m$  is 8.9 J kg<sup>-1</sup> K<sup>-1</sup> under a field change of 0-50 kOe, which is comparable

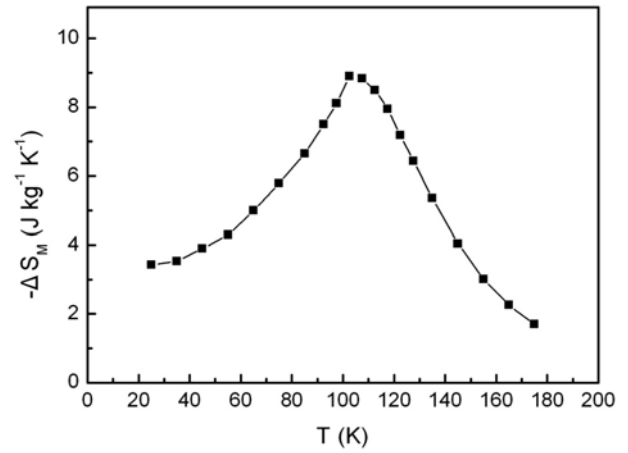


**Fig. 5.** Magnetic entropy change as a function of temperature for Gd<sub>55</sub>Co<sub>20</sub>Al<sub>23</sub>Si<sub>2</sub> BGA under 50 kOe.

with that of Gd<sub>55</sub>Co<sub>20</sub>Al<sub>25</sub>. Additionally, the relative cooling power or refrigeration capacity (RC) is another important parameter for evaluating magnetic refrigerants. According to Gschneidner's method [17], the RC value is calculated by  $-\Delta S_m \times \delta T_{FWHM}$ , where  $\delta T_{FWHM}$  is the full-

**Table 1.** Thermal and magnetocaloric properties of Gd<sub>55</sub>Co<sub>20</sub>Al<sub>23</sub>Si<sub>2</sub> glassy alloy, the data of some other glassy alloys are also shown for comparison.

Materials	$T_g$ (K)	$T_x$ (K)	$\Delta T_x$ (K)	$T_c$ (K)	Field (kOe)	$\Delta S_{\max}$ (J kg <sup>-1</sup> K <sup>-1</sup> )	RC (J kg <sup>-1</sup> )
Gd <sub>55</sub> Co <sub>20</sub> Al <sub>23</sub> Si <sub>2</sub>	600	679	79	105	50	8.9	774
Gd <sub>55</sub> Co <sub>20</sub> Al <sub>25</sub> <sup>11</sup>	594	649	55	105	50	8.8	541
Gd <sub>53</sub> Co <sub>20</sub> Al <sub>25</sub> Zr <sub>3</sub> <sup>4</sup>	603	648	45	93	50	9.4	780
Gd <sub>60</sub> Co <sub>26</sub> Al <sub>14</sub> <sup>10</sup>	550	581	31	79	50	10.1	557
Gd <sub>36</sub> Y <sub>20</sub> Al <sub>24</sub> Co <sub>20</sub> <sup>1222</sup>	603	658	55	53	50	7.76	459
Tb <sub>55</sub> Co <sub>20</sub> Al <sub>25</sub> <sup>19</sup>	614	680	66	45	70	9.75	540

width at half-maximum. In  $\text{Gd}_{55}\text{Co}_{20}\text{Al}_{23}\text{Si}_2$  alloy, the  $\Delta S_m$  and  $\delta T_{\text{FWHM}}$  are  $8.9 \text{ J kg}^{-1} \text{ K}^{-1}$  and  $87 \text{ K}$ , respectively, so the RC is  $774 \text{ J kg}^{-1}$ . In addition, Provenzano *et al.* pointed out that effective refrigeration capacity is the RC that subtracts the hysteric loss [18], but it has been proved there is almost no hysteresis loss for the Gd-based BGAs [11]. Therefore, the  $774 \text{ J kg}^{-1}$  of the RC is the effective refrigeration capacity for  $\text{Gd}_{55}\text{Co}_{20}\text{Al}_{23}\text{Si}_2$  alloy. For comparison, the magnetocaloric and thermal properties of  $\text{Gd}_{55}\text{Co}_{20}\text{Al}_{23}\text{Si}_2$  alloy and some other typical materials are listed in Table 1.

#### 4. Conclusion

$\text{Gd}_{55}\text{Co}_{20}\text{Al}_{23}\text{Si}_2$  glassy alloy with a diameter of 5 mm has been successfully synthesized. It is found that the addition of 2 at.% Si in  $\text{Gd}_{55}\text{Co}_{20}\text{Al}_{25}$  glassy alloy is effective for extension of the supercooled liquid region ( $\Delta T_x$ ). The  $\Delta T_x$  is 55 K for the  $\text{Gd}_{55}\text{Co}_{20}\text{Al}_{25}$  glassy alloy, and increases to 79 K for the  $\text{Gd}_{55}\text{Co}_{20}\text{Al}_{23}\text{Si}_2$  alloy, which indicate a better GFA. Moreover, the alloys also exhibit the larger MCE. The magnetic entropy change ( $\Delta S_m$ ) and the refrigerant capacity (RC) are  $8.9 \text{ J kg}^{-1} \text{ K}^{-1}$  and  $774 \text{ J kg}^{-1}$ , respectively. Therefore, it is expected that this  $\text{Gd}_{55}\text{Co}_{20}\text{Al}_{23}\text{Si}_2$  glassy alloy is an ideal candidate for the magnetic refrigeration application.

#### Acknowledgements

This work was supported by the National Science Fund for Distinguished Young Scholars (Grant No. 50825103) and the “Hundred of Talents Program” (Grant No. KG CX-2-YW-803) by Chinese Academy of Sciences.

#### References

- [1] V. K. Pecharsky and K. A. Gschneidner, Phys. Rev. Lett. **78**, 4494 (1997).
- [2] O. Tegus, E. Bruck, K. H. J. Buschow, and F. R. de Boer, Nature **415**, 150 (2002).
- [3] K. A. Gschneidner, V. K. Pecharsky, and A. O. Tsokol, Rep. Prog. Phys. **68**, 1479 (2005).
- [4] Q. Luo, D. Q. Zhao, M. X. Pan, and W. H. Wang, Appl. Phys. Lett. **89**, 081914 (2006).
- [5] Q. Luo, D. Q. Zhao, M. X. Pan, and W. H. Wang, Appl. Phys. Lett. **90**, 211903 (2007).
- [6] F. X. Hu, B. G. Shen, and J. R. Sun, Appl. Phys. Lett. **76**, 3460 (2000).
- [7] F. X. Hu, B. G. Shen, J. R. Sun, Z. H. Cheng, G. H. Rao, and X. X. Zhang, Appl. Phys. Lett. **78**, 3675 (2001).
- [8] H. Wada and Y. Tanabe, Appl. Phys. Lett. **79**, 3302 (2001).
- [9] M. E. Wood and W. H. Potter, Cryogenics **25**, 667 (1985).
- [10] H. Fu, X. Y. Zhang, H. J. Yu, B. H. Teng, and X. T. Zu, Solid State Commun. **145**, 15 (2008).
- [11] J. Du, Q. Zheng, Y. B. Li, Q. Zhang, D. Li, and Z. D. Zhang, J. Appl. Phys. **103**, 023918 (2008).
- [12] L. Liang, X. Hui, Y. Wu, and G. L. Chen, J. Alloy. Compd. **457**, 541 (2008).
- [13] J. Guo, X. F. Bian, Q. G. Meng, Y. Zhao, S. H. Wang, C. D. Wang, and T. B. Li, Scripta Mater. **55**, 1027 (2006).
- [14] The Japan Institute of Metals, Metals Databook, Maruzen, Tokyo (2004) p.8.
- [15] S. J. Poon, G. J. Shiflet, F. Q. Guo, and V. Ponnambalam, J. Non-Cryst. Solids **317**, 1 (2003).
- [16] F. R. De Boer, R. Boom, W. C. M. Mattens, A. R. Miedema, and A. K. Niessen, Cohesion in Metals, The North-Holland Physics Publishing, Amsterdam (1989) p. 217.
- [17] K. A. Gschneidner and V. K. Pecharsky, Annu. Rev. Mater. Sci. **30**, 387 (2000).
- [18] V. Provenzano, A. J. Shapiro, and R. D. Shull, Nature **429**, 853 (2004).
- [19] J. Du, Q. Zheng, E. Bruck, K. H. J. Buschow, W. B. Cui, W. J. Feng, and Z. D. Zhang, J. Magn. Magn. Mater. **321**, 413 (2009).